ASSESSMENT OF RESIDUAL STRESSES IN FRICTION WELDMENTS OF ALUMINUM TUBES

By

Dr. M.Es. ABDEL MONEIM *, Dr. S. M. SERAG **
Prof.Dr. A. A. NASSER *** and A. A. MOUSTAFA ****

SUMMARY:

In the current paper, some of the fundamentals of friction welding of commercially pure Aluminum tubes are studied.

A center lathe has been adapted to perform the needed welding operation.

A special guiding attachment was designed to fix the stationary part of the pure aluminum tube on to the tool post during welding.

The tested variables were being the spindle speed, tube thickness and the vertical chamfering angle of the tube end.

Residual stresses distribution at the middle section of the weldment were assessed via the layer removal technique.

That technique was employed mechanically via very sharp orthogonal edges in the presence of ample cooling in order to minimize the machining residual stresses.

* Mansour EL-Sayed Abdel Moneim, Dr. Consultant Idustrial Eng.
** Soad Mohamed Serag, Dr., B.Sc. Ph.D. Lecturer, Dept. Prod. Eng. & Technology, Menoufia University, Egypt.
*** Abdel Hady Abdel Bary Nasser, Professor Dr., Dept. Prod.Eng. & Machine Design, Faculty of Eng. & Tech.,Menoufia University.
**** Adel Abdel Aziz Moustafa, Demonstrator, Dept. Prod. Eng. & Tech. Faculty of Eng. & Technology, Menoufia University.

Generally, as the spindle speed increase, the value of the maximum tensile stress and the depth of the stressed layers were found to rise.

As the wall thicknesses of the tube increase so do the level of residual stresses.

However, no significant effect of the vertical chamfering angle was revealed on the residual stresses.

The depths of the stressed layers for all the tests were found to range between 1150 to 13 0 microns which represent a ratio of 0.2 to 0.35 of the tube thickness.

As for the nature of those stresses, they were tensile surface stresses followed by compressive then by tensile stresses. It was found that the area of the tensile stresses would approximate that of the compressive stresses.

INTRODUCTION:

In principle, friction welding is a type of pressure welding. It may be described as a process wherein mechanical energy, through the medium of frictional forces, is converted to thermal energy which in turn heats the two mating surfaces to a proper welding temperature.[1]

In practice, this energy conversion can be accomplished by several methods.

The least complex of these involves the rotation of one of the two parts to be welded at a relatively high speed, while maintaining a compressive axial force on the two parts.[2]

The mating surfaces, thus, receive heat energy until they reach the welding temperature. At this point, the relative motion

between the two parts is stopped-within a fraction of a second-and, while maintaining or increasing the axial force, the interface is allowed to cool, accomplishing the weldment.

Fig. (1) illustrates the simplest and most common scheme for friction welding. Here, two cylindrical bare are axially aligned with one bar rotating.

For steels, the welding temperature should be above the upper transformation temperature.

Fortunately, temperatures up to the melting point (about 1480°C for carbon steels), can be generated easily by friction[2]. Usually molten metal is squeezed out from the interface as the junction form.

The metal at, and immediately behind, the interface is heated to the desired temperature in a matter of seconds enabling sufficient metal behind the interface, to soften permitting the pieces to be joined together. Caution should be exercised for heat treated steels after welding. Such post-heat treatment, if any, will be dependent on the work-piece material type, geometry, and properties as well as the particular welding cycle.

In the course of welding, marked plastic deformation takes place on the surfaces being welded[2].

It is believed that a strong weldment is formed by metallic bonds which arise between the new surfaces of contact.

Surface films and inclusions, that may interfere with the formation of these bonds, are broken up by friction and removed from the welding area. Those films go away in radial directions[3].

To bring about the necessary deformation, the metal soften by the frictional heat generated confined onto the thin surface layers.

The friction forces of the mating surfaces do increase as their relative rotational speed rise.

The work done to overcome those forces, usually, is converted into heat. That energy is to be liberated at the rubbing surfaces increasing rapidly the metal temperature up to the appropriate welding temperature.

The metallic layers being heated are, usually, so small that the heating cycle consume a very short time interval, less than 30 seconds.[3]

EXPERIMENTAL DETAILS

A rigid lathe (type DLZ 450/I) of the specifications given in table (II-1) was employed throughout the welding tests.

Table (II-1): The main specification of the employed lathe.

Motor Power and Speed	10.3 K.W., 3000 R.P.M.
Spindle speeds:	16,45,31.5,90,22.6,63,100,280,200,560. 140,400,1120,800,2240,560,1600 R.P.M.
Distance between centers	152 cm.
Height over bed	225 mm.
Max. diameter of workpiece.	450 mm.

Feeds: Range 0.08-1.12 mm/rev.

Infeeds: Range 0.036-0.5 mm/rev.

The objective behind the use of the lathe is to rely on available machine to be found in any worksnop in order to perform the friction welding.

Slight modification or in other words some additional means had to be designed to ensure proper fixation of the workpieces during the welding process. Many trials in vain had been made to fulfill such objective. Firstly, an attachment as shown in Fig. (1) was designed and manufactured.

However, digging was noted on the surface of the work pieces due to an unavoidable and uncontrolable clamping forces.

Moreover, no room was left to perform the necessary measurements. An alternative attachment as outlined in Fig. (2) was, hence, designed. Such arrangement was found to be inadequate, yielding non uniform motion of the two workpieces to be joined by welding. Finally, a better sound design for that attachment was arrived at. That arrangement is shown in Fig. (3). That attachment is composed mainly of two parts held together via a pin.

The first part is shown in Fig. (4). That part serve as a sleeve for the second part. The former part is fixed via a welded flange onto the toolpost.

The second part shown in Fig. (5) is a housing to the stationary workpiece. The end of the second part is slotted axially and provided by a pair of flanges at each side. These flanges are welded to the frontal portion of the second part. They are utilized as a fixture of the stationary part.

All the workpieces were made of commercially pure aluminum (99.6%). The ingots were turned and hollowed via drilling and fine turning techniques. The initial workpiece outside, diameter was around 42 mm. Tubes thicknesses were varied between 4 to 7 mm. Their lengths were around 50 and 80 mm. for the rotary and stationary work pieces respectively. As far as the measurements are concerned, attention was directed towards the assessment of the residual stress distribution within the welded work piece at the end of the test.

Friction welding tests were performed according to a novel technique employed, here for the first time.

The Employed Friction Welding Technique:

Axis alignment for the two tubes to be welded was to be ensured for each test. While one of the tubes was fixed to its attachment, at the tool post; the other was to be held at the lathe chuck. The lathe was derived at prescribed speed. The manual longitudinal feed wheel was rotated manually about $2\frac{1}{2}$ times to ensure proper approachment of the two tubes.

That wheel motion was to be stopped as soon as the radial upset flow begin to appear. The initial feed motion approximate for each test, on the average, about 2 mm. Afterwards, the lathe power was to be disengaged and the spindle motion cease gradually. Later on, and while the rotary movement decay and as soon as the stopping lever of the machine is activated, another secondary manual longitudinal feed begin. Such feed was adjusted to act as a further brake to ensure positive solid weld. That implies more feed force (found to approximately twice that needed for the primary feed (movement). Attention should be paid, here, to the fact that the increase of the force is to be attributed to the additional force required to speeden the spindle stopping action as well as to the force necessary to complete the weld. As the spindle stop, so the left ward movement of the nonrotary part of the welded workpiece (that tube fixed to the tool post of the lathe). That represent practical, repeatable way of performing the required friction weldments.

The welded tubes was, then, allowed to cool to the room temperature, at least for one hour. That was sufficient in every case to ensure stability temperature of the finisned tube at the room temperature, judging, simply by touching.

As far as the residual stresses measurements are concerned, the change of the overall length, was taken as an index. (See Fig.6). Appendix (1) outline the residual stresses computation formula.

The Employed Residual Stresses Assessment Technique:

The welded tube was then removed off the lathe and its attachment to the tool post (the workpiece jig was dismantled). The finisned welded tube was then fixed to the lathe chuck. Firstly, the tool post was employed to internally turn the tube via sharp internal tools. The infeeds were taken to be as small as possible in the very wet conditions (via a soluble cutting fluid). Such steps were taken to practically avoid the introduction of any further residual stresses to truly represent that of the welding.

Afterwards, external sharp cutting tools were employed to remove the outer upset of the welded friction junction. That was performed upon fixing the external turning tool on its post. Light cuts were taken in the very wet condition to avoid the complexity of superimposed residual stresses.

The welded tubes was, then, fixed to its mandrel (see Fig.6).

In order to assess the residual stresses; the layer removal technique was employed via machining.

The machining was performed via cutting tools held on the tool-post. Caution was exercised to minimize the additional residual stresses caused by the machining itself. That was done by utilizing very sharp orthogonal tool which would be cleaned from now and then to remove the probable built-up edge formation. Machining was done in the presence of suitable cutting fluid. The machining speed to remove the work piece stressed layers in steps was around 100 mt/min. The feed was chosen to be 0.06 mm/rev. The infeed was around 0.05 mm.

The welded tube was, then, fixed to its mandrel (See Fig.6).

Tube length changes between the recesses were taken as the average of three readings at different positions located 120° apart around the tube contour. Such positions were indexed utilizing the three jaws chuck of the lathe.

Later on, layers removal were repeated in order to obtain the overall distribution of the residual stresses via the layer removal technique. Appendix (1) gives the residual stresses computation formula due to Tadasni[5].

The tests were done in three sets. During the first set, the speed of rotation is the variable while the others were kept constant.

Table (2)

Rotational speeds: 2240, 1600, 1120, and 800 r.p.m.

d_o = 42 mm

d_i = 30 mm

= 45° (For 3 mm width)

t = 6 mm

In the second set, the vertical chamfering angle is the variable while the others were kept constant.

Table (3)

Chamfering : 15°, 30°, 45° and 60° (For 3 mm width)

r.p.m. = 1600 mm

d_o = 42 mm

d_i = 30 mm

t = 6 mm

In the third set, the tube thickness is the variable while the others were taken constant.

Table (4)

Thickness (t)

t = 4,5 and 6 mm

r.p.m.= 1600 mm

= 45° (For 3 mm width)

d_o = 42 mm

d_i = 34, 32 and 30 mm respectively.

EXPERIMENTAL OBSERVATIONS

The utilized bars were found to be free of structural defects. However, out of roundness were noted for the stock. Such irregularities were removed by light machining to avoid the introduction of residual machining stresses, via the initial preparatory turning operations. That would minimize the possibility of the existence of pre-welding residual stresses. In order to en-hallow the bars, drilling operations were necessary at the initial preparatory stages. These were carried out, firstly, via large drill diameters. However, large amounts of heat generations and higher degrees of material plastic flow were noted. That was thought to be unrecommended, since the reliance on large drills, at the beginning, would lead eventually to higher levels of initial residual stresses.

Such via was therefore altered and small drills were employed instead to avoid that serious problem. Moreover, adequate cooling, small feed and speed were employed to ensure, to the best, bars on the as-recieved condition as for the level of residual stressses.

Tube chamfering was performed at the ordinary high cutting speed of aluminum. Although this approach avoid the built-up edge formation, alas this may lead to residual stress if large amounts of heat generation are liberated during the machining. This was lessened via amble flow of the cutting fluid during the machining operations.

High level of machine carriage vibrations was noted firstly. That may be attributed to two main reasons, 1) High welding pressure at larger rotary spindle speed, 2) Any clearance existing of the carriage ways.
Those reasons are hard to be removed due to the intrihsic nature of the friction welding and to the reliance on an ordinary lathe. The later reasoning was intentional since a practical available means for friction welding utilizing the common machine shop lathe

was one of the objective of the current research.

However, the vibration of the carriage was eliminated by fixing it to the latne bed.
Rather than advancing the entire carriage: the stationary (non rotating) part was advanced via the advanced compound rest of the lathe.

As the stationary part touch the rotary part at the beginning of the friction welding process high level of noise was heard. This may be attributed to severe rubbing action as the sharp edge asperities getting touch.

Later on little amount of smoke was viewed at the welding zone.
This is understandable since the sharp edges of the asperities of the mating surfaces would rapidly,fractured and the actual contact area would increase leading to a nigher heat generation.
That is to say the initial severe rubbing action of the sharp asperities would immediately be substituted by severe friction action of fractured asperities of the mating surfaces.
Then one could expect noise followed by smoke.

At the conclusion of the welding, the welded tube was to be removed in order to assess the residual stresses.

Sinde flow was usually noted upon layer removal on the sides of the recesses which were prepared as references for the length changes. That is attributed to the lack of non plane strain condition. This violation take place in metal cutting due to many reasons.

It was noted in the current research that violation increase as the feed and infeed rise. Since the crucial factor was the infeed rate; it was decided to decrease that factor practically as much as possible keeping in mind that such decrease would lead to more sensitivity in residual stresses assessment.

Filling the sides of those recesses, lightly, was proven to be useful to clean those recesses for length change measurements.

EXPERIMENTAL RESULTS AND DISCUSSION:

Following are the results and their discussion arranged according to the different experimental sets.

First set:

In that set all factors were kept constant except the spindle speed (N). Keffering to Fig. (7) through 10) it can be seen that:

1) The maximum longitudinal residual stress (σ_z) was found to be quite close to the very surface of the welded tube and to decrease in magnitude as the rotational speed decrease (See Fig. (11). That value was found to vary between 0.4 to 0.6 of σ_y.

2) At the spindle speed decrease, the longitudinal residual stress (σ_z) vary between maxima and minima values.

3) There are certain locations whereas the values of the longitudinal residual stress vanish. More than one location for each employed rotational speed (N) were encountered. The first location of that null longitudinal residual stress was found to be at a subsurface depth (X) of about 0.40 mm. Generally, the other locations were found to go away deeper underneath the surface of the tube as the rotational speed become greater.

4) The magnitude of the minimum residual stress has no clear correlation with the rotational speed.

5) There are more than one inflection location. At those locations the longitudinal residual stress comes to minima and become compressive.

6) At around 0.50 mm of the outer surface of the tube one can get the first location for the minimum longitudinal residual stress.

7) Generally, as the rotational speed (N) becomes greater; the last location of the minimum residual stress becomes more deeper, away of the welded tube outer surface.

8) Refering to Fig. (11); it can be seen that as the rotational speed increase: the maximum depth of stressed layer (X_{max}) increase. Peculiar increase at the lowest employed rotational speed was noted.

Second Set

In that set all factors are kept constant except the tube chamfer angle (α). Refering to Figs. 8,12,13 and 14: one can deduce the following:

1) As the chamfering angle change no significant alteration on neither the value of the maximum longitudinal residual stress (σ_{max}) (found to be about 3.9 kg/mm^2 on the average) nor its location (found to be quite close to the very surface) were noted (see Fig. (15)).

2) No alteration was found to take place on the maximum depth of the stressed layer (found to be about 1.22 mm) upon the chamfering angle (α) change (see also Fig. (15)).

3) As the chamfering angle increase; the location of the first position whereas the longitudinal residual stress vanish become nearer to the welded tube outer surface.

4) Generally as chamfering angle (α) increase: the location of the last position of zero longitudinal residual stress become nearer to the outer surface.

5) As the chamfering angle (α) increase from 15° to 45° the value of the maximum compressive longitudinal residual

stress was from -3.15 Kg/mm^2 to -4.5 Kg/mm^2. However, such trend reverse for further increase of the chamfering angle to 60°. At that angle the maximum compressive longitudinal residual stress is -3.2 Kg/mm^2.

Third Set

In that set the tube thicknesses were varied with the rest of the factors were kept constant. Refering to Fig. 8, 16 and 17, one can deduce the following:

1) As the wall thickness of the tubes decrease, the maximum tensile longitudinal residual stress were found to increase termindously. Its value was found to vary between 0.5 to 0.8 σ_y of the material. That is best manifested by Fig. (18).

2) That maximum residual stresses were found to be located at the very outer surface, nearly.

3) As for the other sets the residual stress goes from tensile longitudinal residual stress to compressive ones. That trend reverse as the distance from the surface become greater. However, lesser vallys; whereby minimea in magnitude of compressive residual stress exist.

4) No significant changes in the location of the first position whereby no residual stress exist were noted as the wall thickness increase.

5) However, as the wall thickness increase, the location or last position of non residual stresses, hence free of strain position; becomes nearer to the outer surface.

6) The value of the maximum compressive longitudinal residual stresss was found to be about 0.6 σ_y or the aluminium specimen. The former amount was found to be insensitive to the alteration in the tube thickness.

7) The depth of the stressed layer, within the welded junction, was found to increase as the welded tube wall thickness

increase. That is recorded also in Fig. (16).

CONCLUSION:

1) The presented attachment for holding the aluminium tubes during welding is valid in the sense that it produced workplaces free of vibration with no surface digging.

2) The employed method for the assessment of residual stresses via the removal technique by finish turning for layers within 50 microns appears to be reliable and quite satisfactory for similar experiments for aluminum specimens.

3) It should be noted that the chemical means for removing aluminum layers via either sodium hydroxide or concentric hydrochloric acid gave uncontrollable results and proved to be impractical.

4) Within the weldment the longitudinal residual stress prove to be of tensile nature at the outer surface upto depths around 350 microns. That zone is denoted, as the first region.

5) Beyond that stressed layers; the residual stress become of compressive nature and go through more than one peak. That zone is denoted, in turn, as the second region.

6) Afterwards and within the third region, the nature of the longitudinal residual stress change to tensile, once more. That change at depths of between (750 to 1270 microns) for the tested weldments.

7) The extent of that third region is the lowest among the triple stressing layers.
Invariably, the areas under the null residual stress axis, for all the conducted tests, were found to approximate that above the line. That is mandatory for an externally balanced component to have residual compressive stresses compensating the residual tensile stresses.

8) The depths of the overall stressed layers range between (1150 to 1350 microns). The represent ratios between (0.2 to 0.35) of the tube wall thickness).

APPENDIX (I)

ASSESSMENT OF RESIDUAL STRESSES DISTRIBUTION IN FRICTION WELDMENTS OF ALUMINUM TUBES.

Reliance has been made on a theoretical treatment presented by Mishimura [5], for the afore-mentioned purpose.

One of the problems in residual-stress analysis has been the development of a method for determining the triaxial residual stress components in a solid bar by measurements of changes of length[5].

That investigation (5) was carried out to develop new equations for the calculations of axisymmetric residual stresses in cylinders in the radial, circumferential and axial directions.

In that analysis obtained in (5), the following assumptions are used:

1) the material is isotropic and its Young's modulus and Poisson's ratio are constant.

2) The deformation due to removal of layers of material is elastic.

3) The stress and strain distributions are symmetrical about the axis of the specimen and constant in the longitudinal direction.

These assumptions lead to relationships among the three res-residual-stress components.
The equations for calculating the residual stresses are derived by employing these relationships and the equation relating the residual stresses to the measured axial strain out of length changes (5).

Consider a long hollow cylinder with an outer radius (b) and inner radius (a). Under conditions of plain streain and axial

symmetry and in the absence of body forces, the equations of equilibrium in cylindrical coordinates reduce to the following form according to Ref. (5):

$$\frac{d\sigma_r}{dr} + \frac{\sigma_r - \sigma_\theta}{r} = 0 \qquad \text{.....(1)}$$

This equation holds for radius as well as for r.

Residual stresses at radius r may be considered as the sum of two stresses when layers of material are removed from radius (b) to radius

$$\begin{aligned} \sigma'_r(r) &= \sigma_r(r) + \sigma''_r(r) , \\ \sigma'_\theta(r) &= \sigma_\theta(r) + \sigma''_\theta(r) , \\ \sigma'_z(r) &= \sigma_z(r) + \sigma''_z(r) . \end{aligned} \qquad \text{.....(2)}$$

Where σ'_r, σ'_θ and σ'_z are the stresses remaining after removal and σ''_r, σ''_θ and σ''_z are the total stress changes caused by the removal.

The unknown stresses σ''_r and σ''_θ can be related to the original radial stress at radius by applying the formulas for a thick-walled cylinder subject to uniform external pressure due to Timoshenko and Goodier[6] ;

$$\begin{aligned} \sigma''_r(r) &= \frac{(r^2 - a^2)\rho^2}{(\rho^2 - a^2)\, r^2}\, \sigma_r(\rho), \\ \sigma''_\theta(r) &= \frac{(r^2 + a^2)\rho^2}{(\rho^2 - a^2)\, r^2}\, \sigma_r(\rho) \end{aligned} \qquad \text{.....(3)}$$

The unknown stress σ_z is assumed here to be uniformly distributed over the cross section $\pi(\rho^2 - a^2)$.

The stress σ''_z can be expressed by integrating the original axial stress present between b and ,

$$\sigma''_z(r) = \frac{2}{\rho^2 - a^2} \int_\rho^b \sigma_z r \, dr \qquad \text{.....(4)}$$

The elastic strains ϵ_r and ϵ_θ present initially at radius (r) may be changed to $\epsilon'_r(r)$ and $\epsilon'_\theta(r)$ when layers of material are removed from radius (b) to radius (ρ). These elastic strains

are transformed into the stresses (σ_r, σ_θ and σ_z) by using the generalized Hook's law, and by substituting eqs. (2), (3) and (4), the following expressions are obtained[6]:

$$\epsilon_{r\rho}(r) = \frac{1}{E}\left\{\sigma_\theta(r) - \frac{(r^2 - a^2)\rho^2}{(\rho^2 - a^2)\, r^2}\ \sigma_r(\rho)\right.$$
$$-\nu\left[\sigma_z(r) + \frac{2}{\rho^2 - a^2}\int_\rho^b \sigma_z(r)\ dr\right.$$
$$\left.\left. + \sigma_\theta(r) - \frac{(r^2 + a^2)\rho^2}{(\rho^2 - a^2)\, r^2}\ \sigma_r(\rho)\right]\right\} \quad \ldots\ldots(5)$$

$$\epsilon_{\theta\rho}(r) = \frac{1}{E}\left\{\sigma_\theta(r) - \frac{(r^2 + a^2)\rho^2}{(\rho^2 - a^2)\, r^2}\ \sigma_r(\rho)\right.$$
$$-\nu\left[\sigma_z(r) + \frac{2}{\rho^2 - a^2}\int_\rho^b \sigma_z(r)\ dr\right.$$
$$\left.\left. + \sigma_r(r) - \frac{(r^2 - a^2)\rho^2}{(\rho^2 - a^2) r^2}\ \sigma_r(\rho)\right]\right\} \quad \ldots\ldots(6)$$

Later on, Nishimura[5] assumed, incorrectly, that the radial displacement at a new surface after removal of the surface layer of thickness.

However, it was proved[5] that the axial stress component can be obtained by the following equation:

$$\sigma_z = -\frac{E}{2(1-\nu)}\left\{\frac{(1-\nu)\rho^2 + (1+\nu)\, a^2}{\rho} \cdot \frac{2\rho\, e_z\, (\rho^2 - a^2)}{(1-2\nu)\rho^2 + a^2}\ e'_z\right.$$
$$\left. + 8\nu^2\ a^2 \int_\rho^b \frac{r\, e_z}{\left[(1-2\nu)\, r^2 + a^2\right]^2}\ dr\right\} \quad \ldots\ldots(7)$$

NOMENCLATURE:

a, b	Inner and outer radii.	(mm)
E	Young's Modulus.	(Kg/mm^2).
e_z	Measured Longitudinal Strain.	(mm/mm)
e'_z	Derivative of Measured Longitudinal Strain.	$(mm)^{-1}$
r	Arbitrary Radius	(mm)
$\epsilon_{(r)}$	Original Elastic Strain at radius (r)	(mm/mm)
ν	Poisson's Ratio.	
ρ	Outer Radius of a cylinder after Removal of a layer.	(mm)
$\sigma_{(r)}$	Longitudinal Residual Stress.	(Kg/mm^2)
$\sigma_{z(max)}$	Maximum Longitudinal Residual Stress.	(Kg/mm^2)
σ_y	Static Tensile Yield Stress.	(Kg/mm^2)
x	Depth of the Stressed Layer.	(micron)
$x_{(max)}$	Total depth from the surface of the stressed Layer.	(micron)

REFERENCES:

1. V.I. Vill, "Friction Welding of Metals, Mashigiz, Moscow - Leningrad, 86 pp (1956). Translated from Russian, A.W.S.(1962).

2. A.L. Phillips, "Welding Hand Book", American Welding Society, Part 3 - Chapter 52, 1964.

3. A.L. Phillips, "Welding Hand Book", American Welding Society, Part 2 - , 1964.

4. G. Nikolaev, N. Olshansky, "Advance Welding Processes", Mir Publisher, Moscow, Chapter 7, 1977.

5. Tadashi Nishimura, "Analysis of Axially Symmetrical Residual Stresses in Bars and Tubes", Experimental Mechanics, May 1978, pp. 180-184.

6. S. Timosnenko and J. Goodier, "Theory of Elasticity"; McGraw-Hill Book Co., New York, 1951, pp. 59-60.

LIST OF FIGURES:

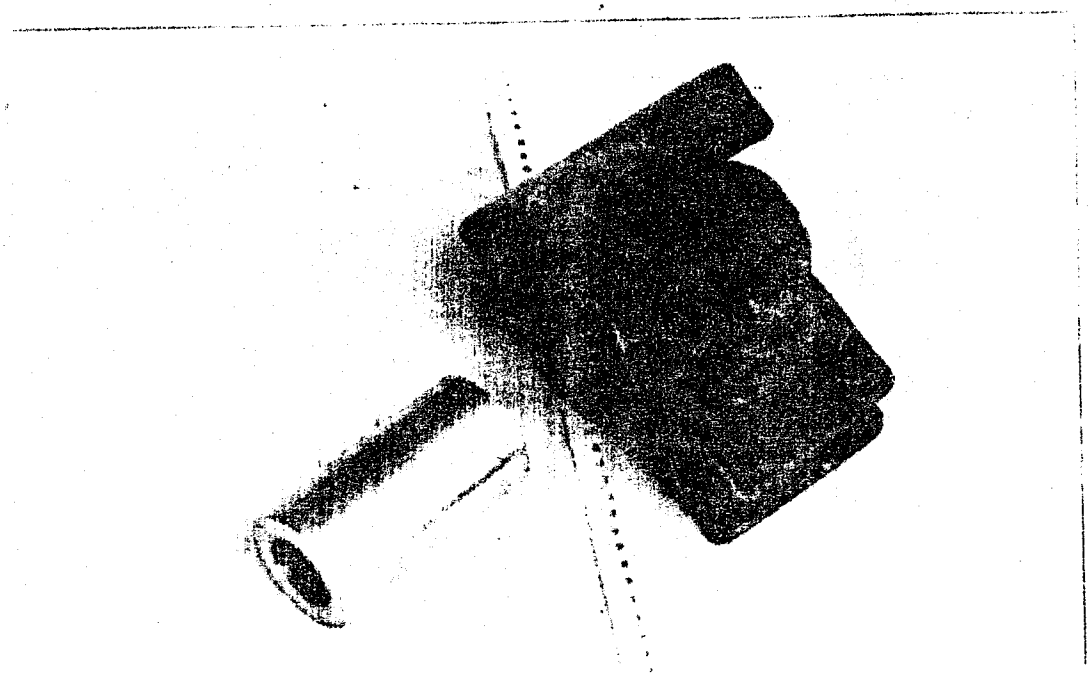

Fig. (1) First Trial for the Welding Fixture.

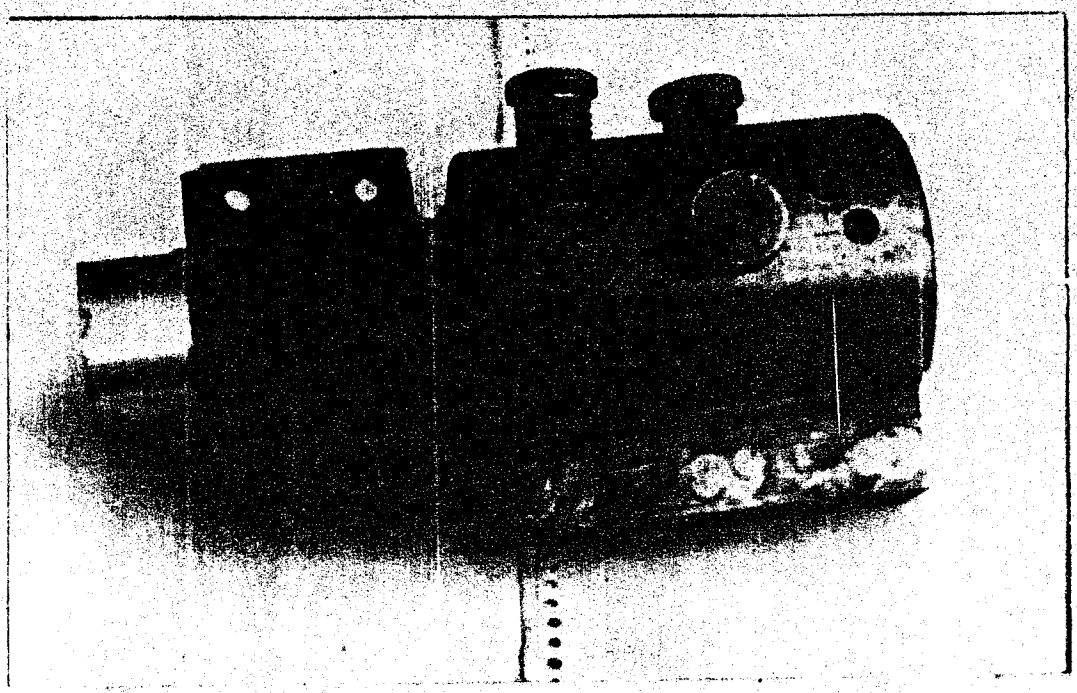

Fig. (2) Second Trial for an alternative Design of the Welding Fixture.

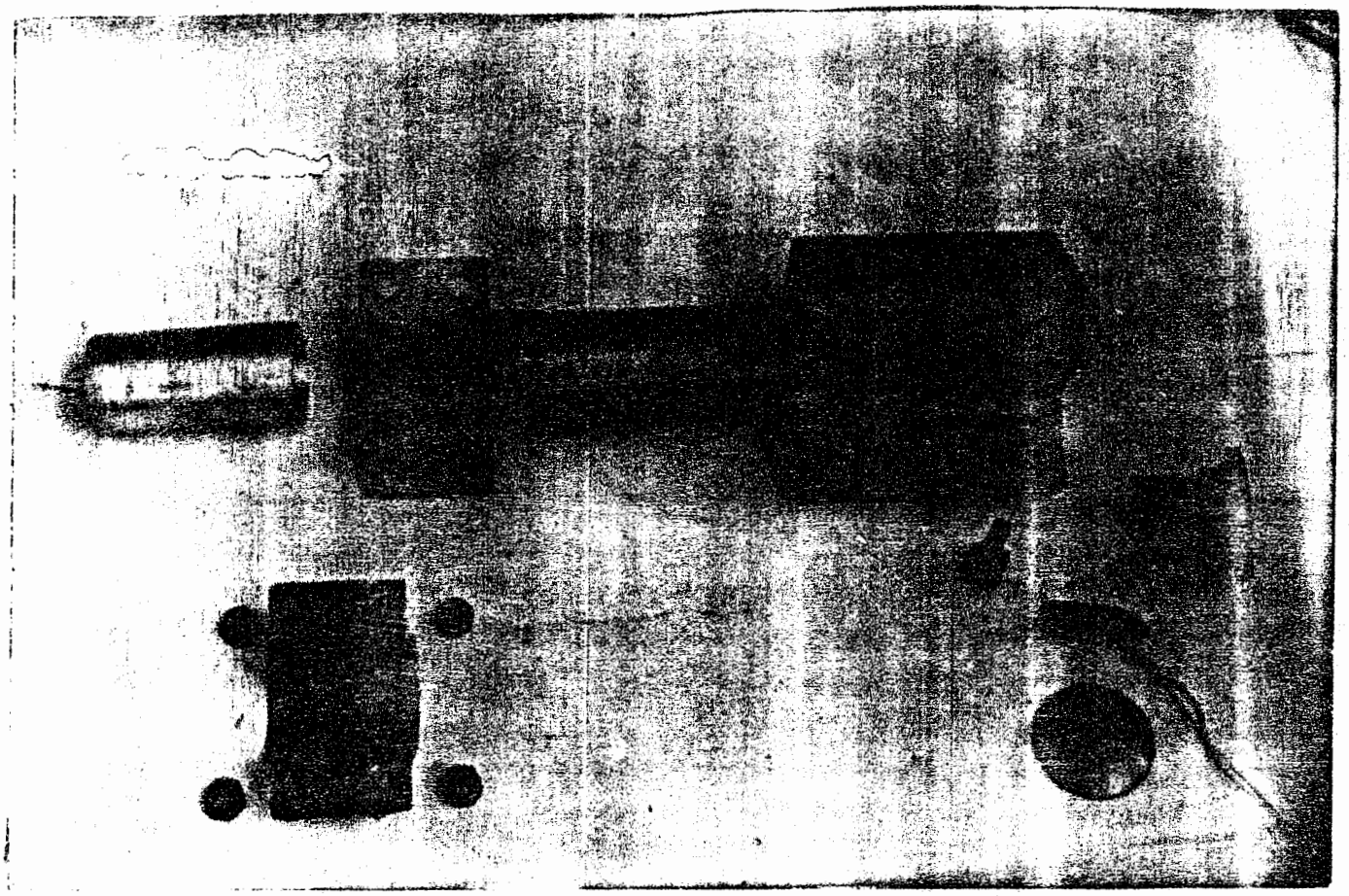

FIG. (3): THE EMPLOYED WELDING FIXTURE.

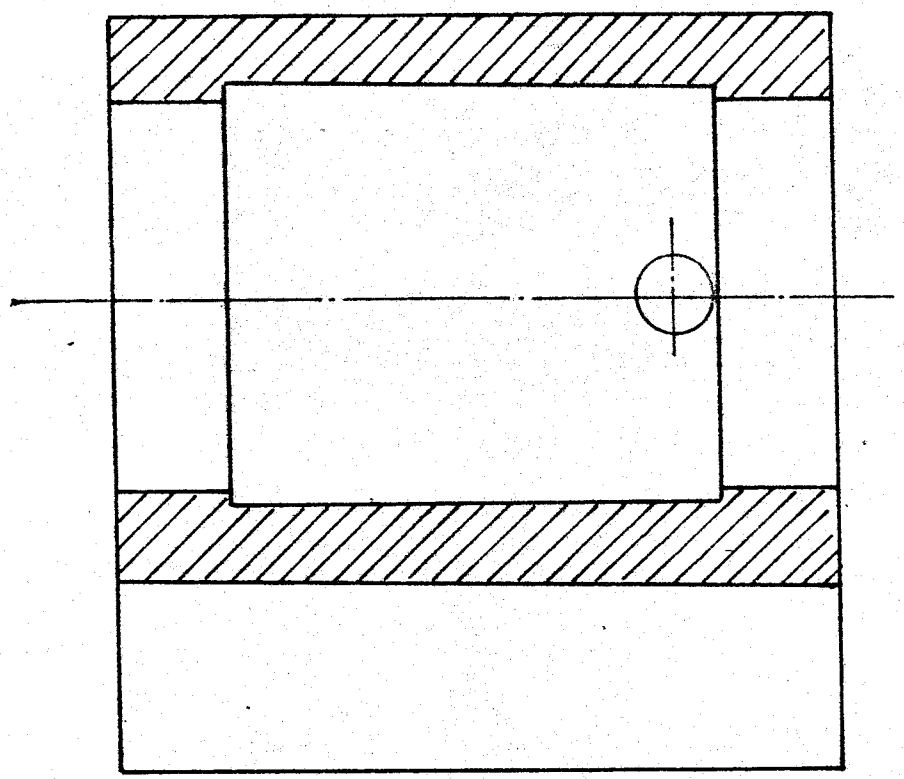

Fig. (4) Fixture for the Sleeve of Aluminum Stationary Tube.

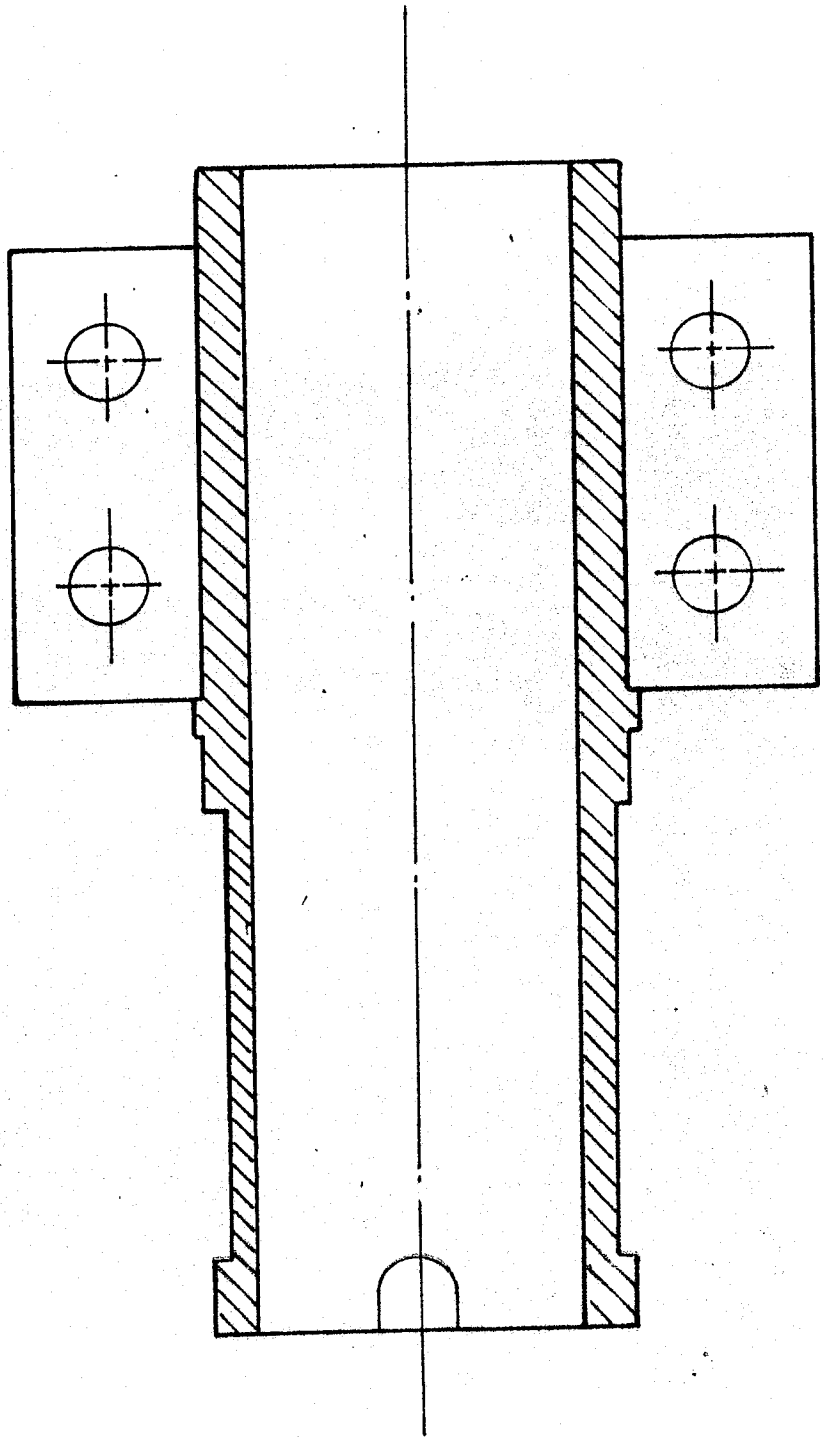

Fig. (5) The Sleeve for the Aluminum Stationary Tubes.

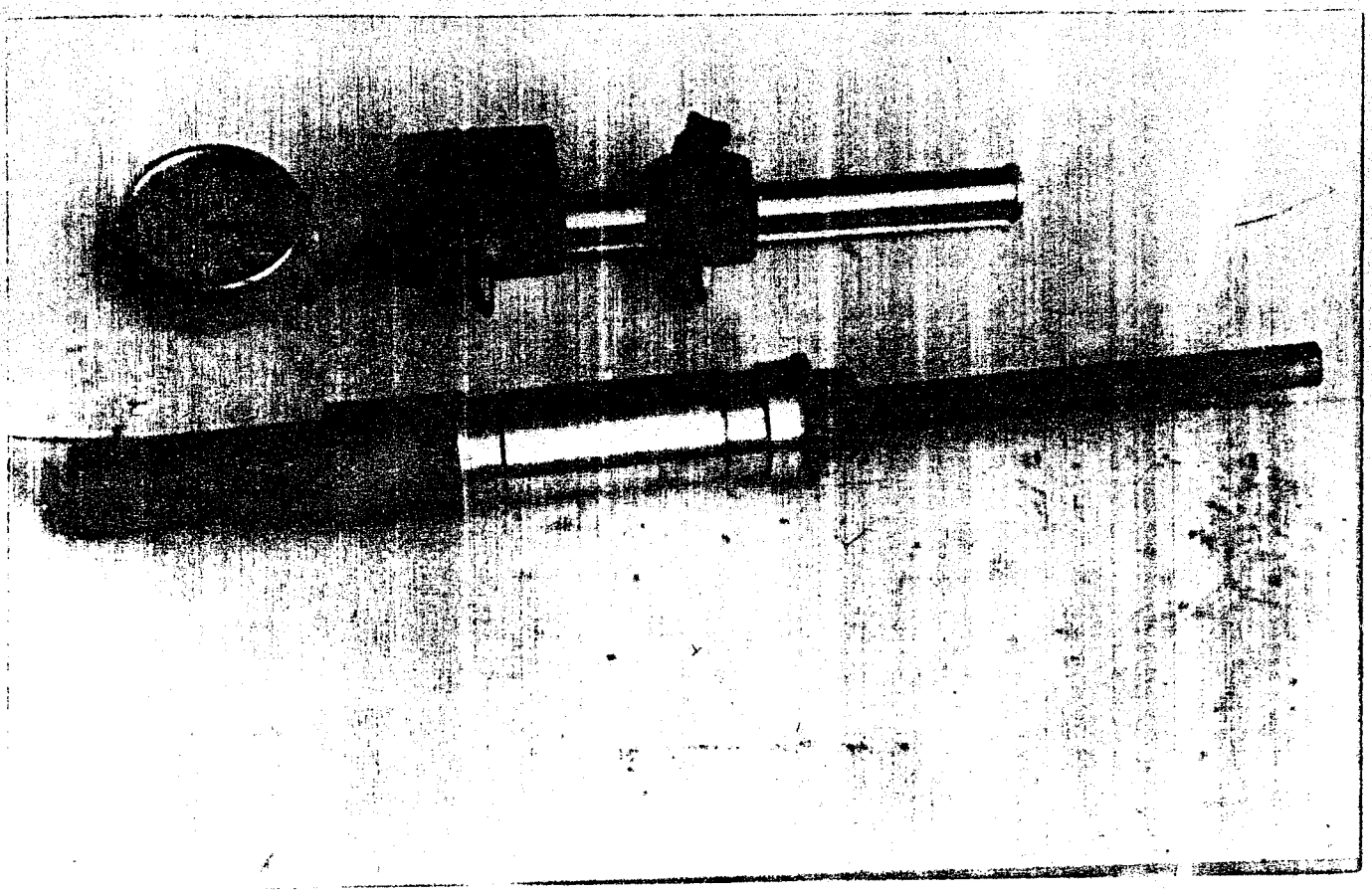

Fig. (6) Mechanical length Comparator and the Residual Stress Mandrel.

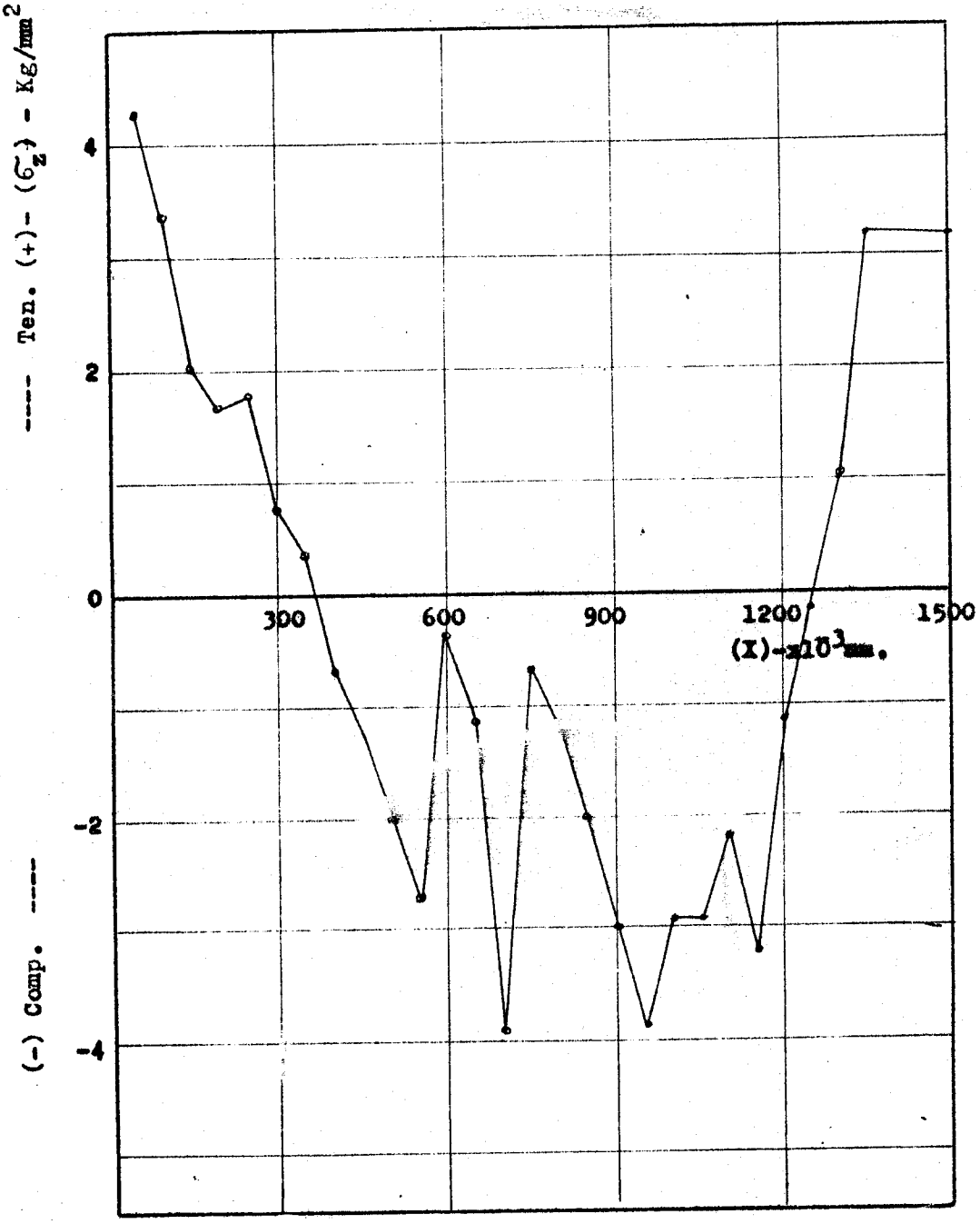

Fig.(7) Longitudinal Residual Stress, (σ_z) Vs. Sub-Surface Depth, (X)-x 10^3 mm. For N = 2240 R.P.M., $\alpha = 45^\circ$ and t = 6mm.

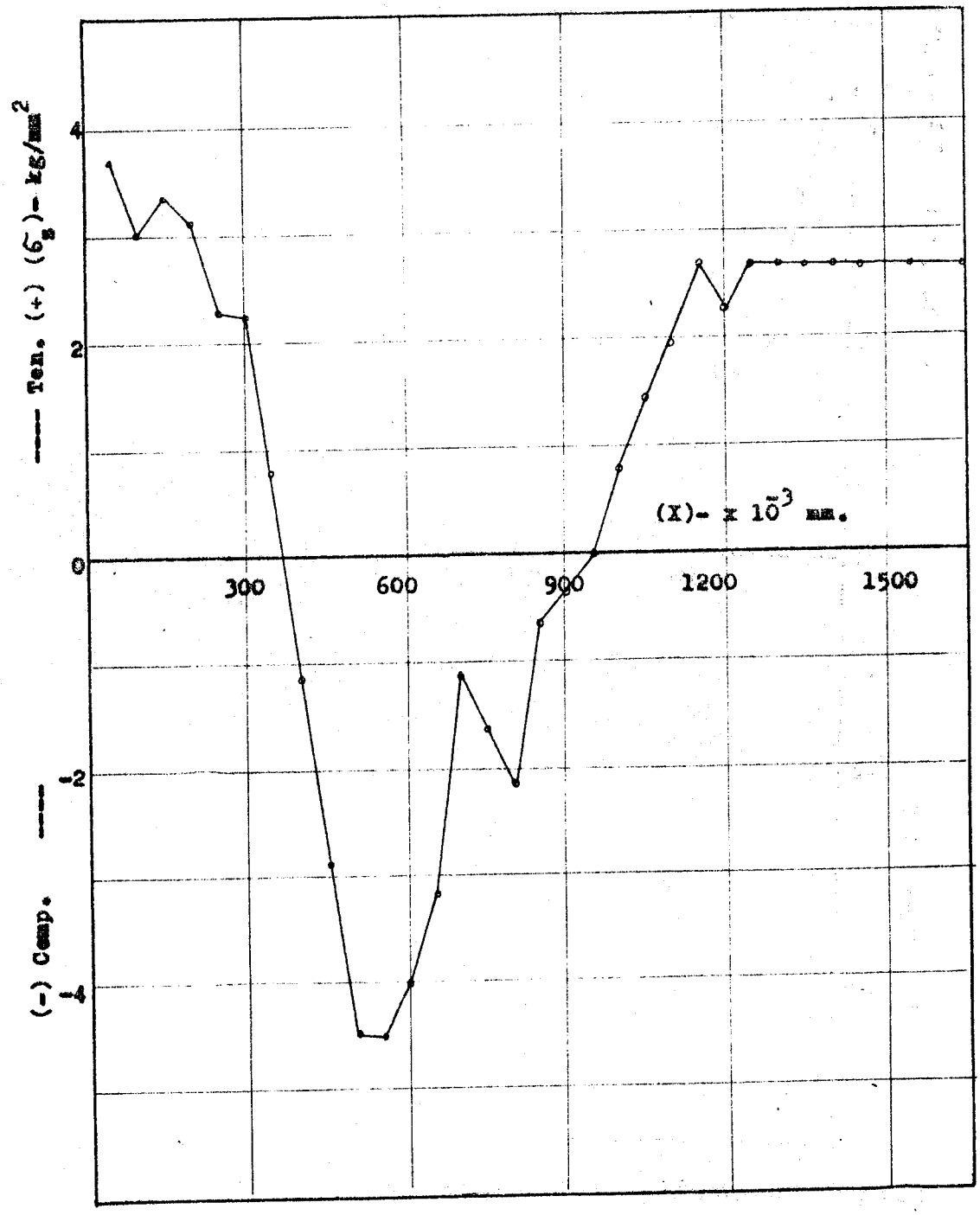

Fig. (8) Longitudinal Residual Stress, $(\bar{\sigma}_g)$- kg/mm^2 Vs. Sub- Surface, (X)- x 10^{-3} mm. For $t = 6$ mm, $N = 1600$ R.P.M. and $\alpha = 45^0$

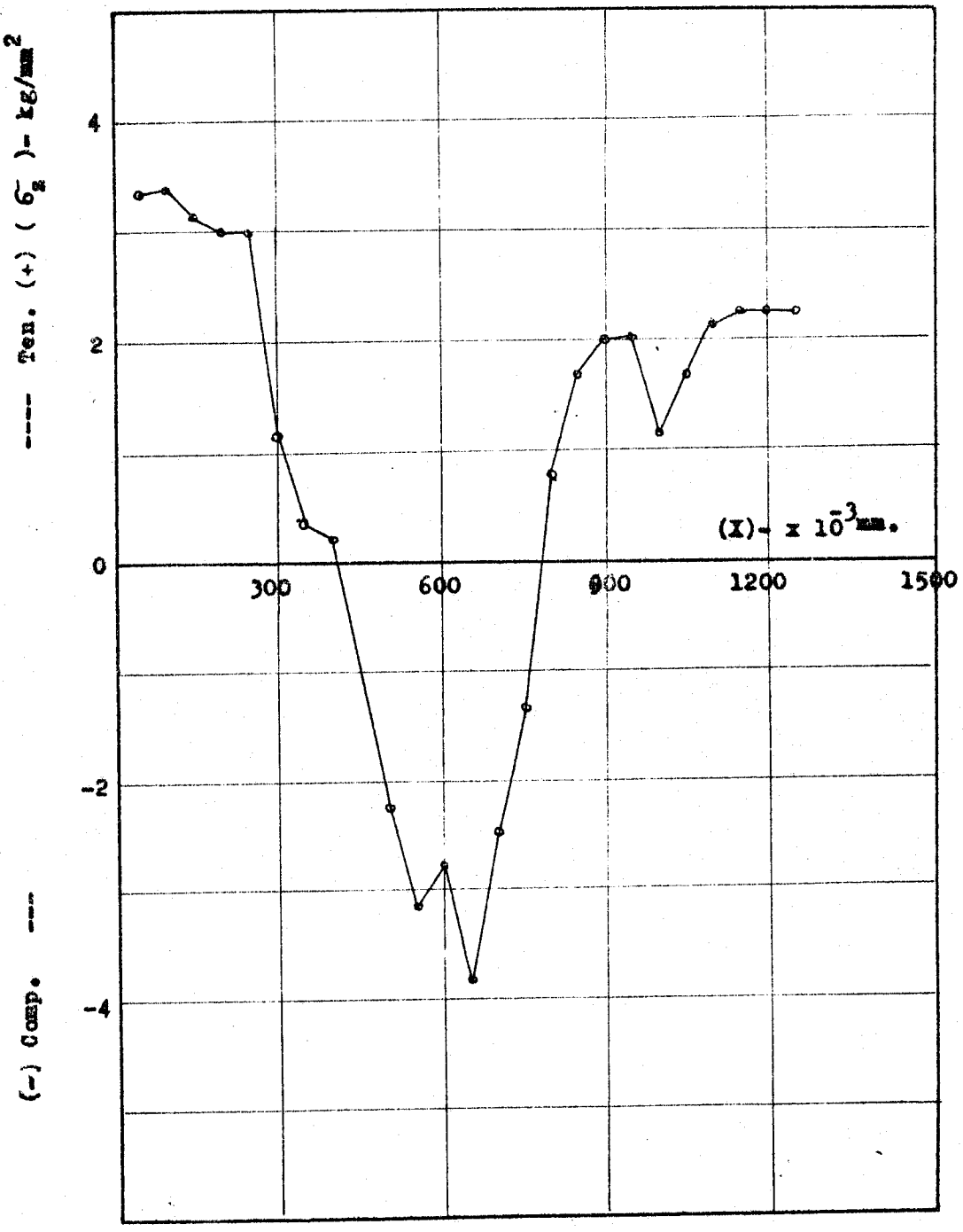

Fig. (9) Longitudinal Residual Stress, ($\bar{6}_z$) Vs. Sub-Surface Depth, (X)- x 10^{-3}mm. For N = 1120 R.P.M., $\alpha = 45^{\circ}$ and t = 6 mm.

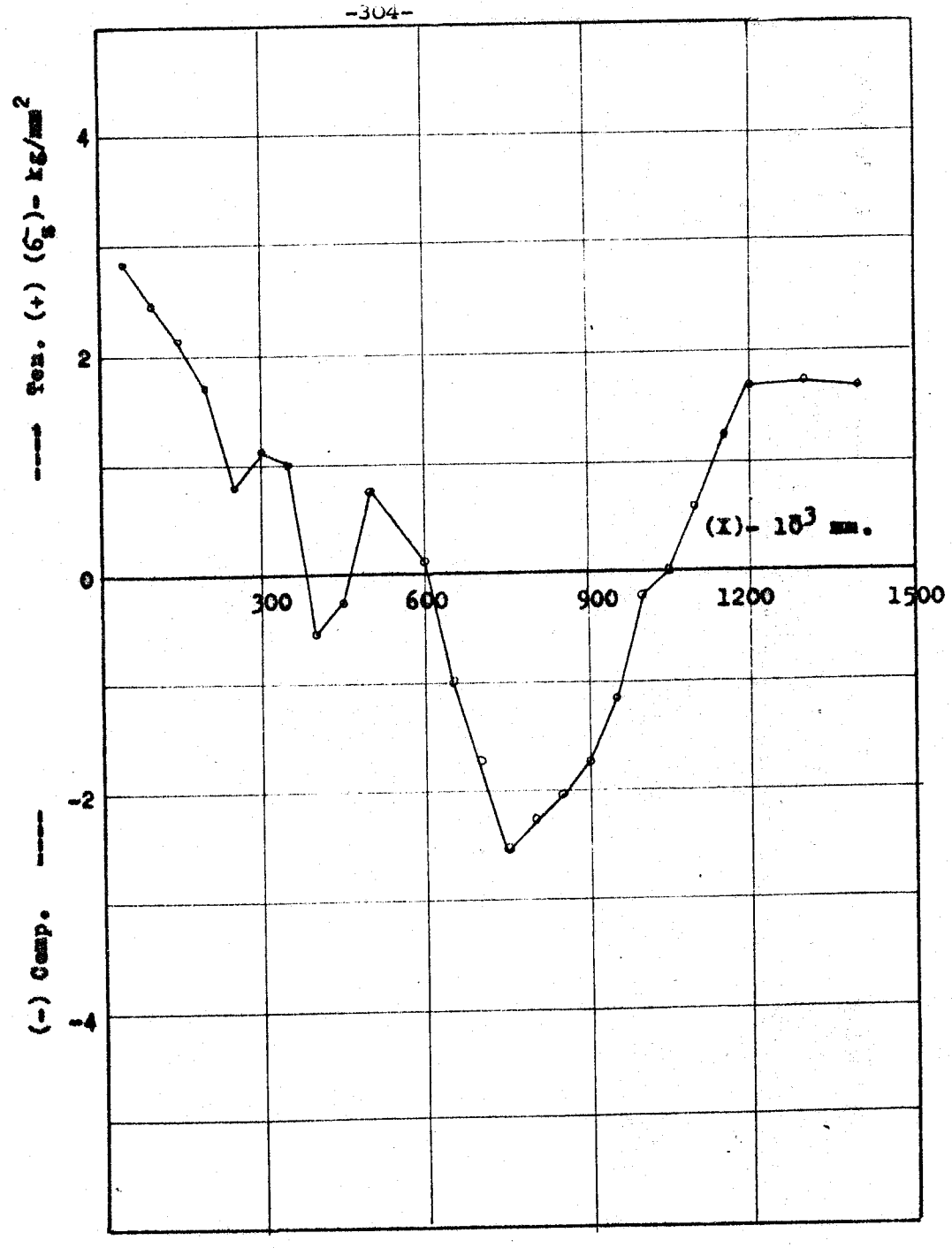

Fig. (10) Residual Stress, (σ_s)- kg/mm^2 Vs. Sub-Surface Depth, (X)- 10^{-3}mm. For N = 800 R.P.M., $\alpha = 45^0$ and t = 6mm.

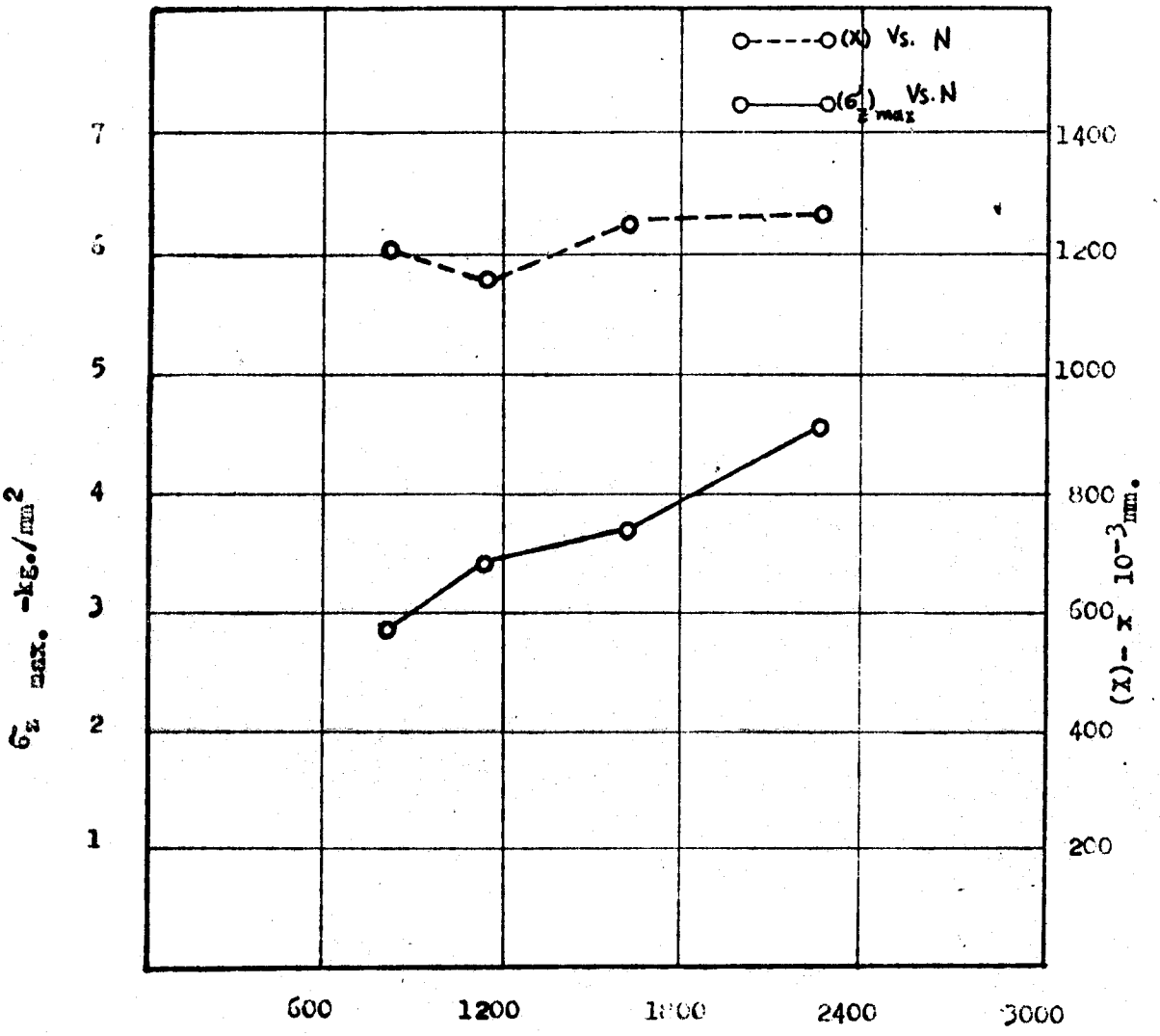

Fig. (11) Variation of the maximum Residual Stress, (σ_z) max. - Kg./mm^2 and the Stressed Layer, (X) - x10^{-3} mm. with Rotational Speed, (N)- R.P.M.

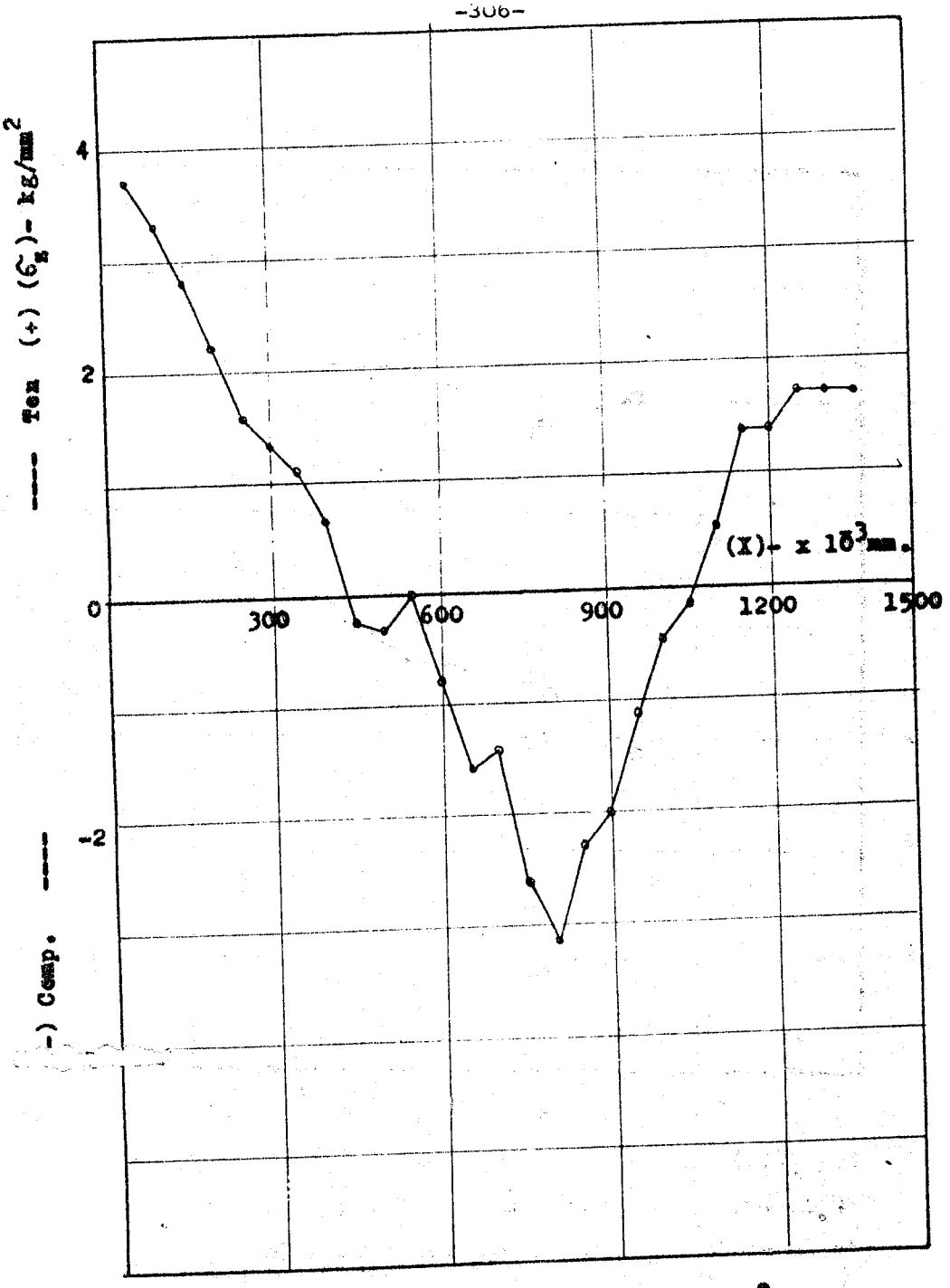

Fig. (12) Longitudinal Residual Stress, (σ_x)- kg/mm^2 Vs. Sub-Surface Depth, (X)-10^{-3}mm. For α = 15° , N = 1600 R.P.M., and t = 6mm.

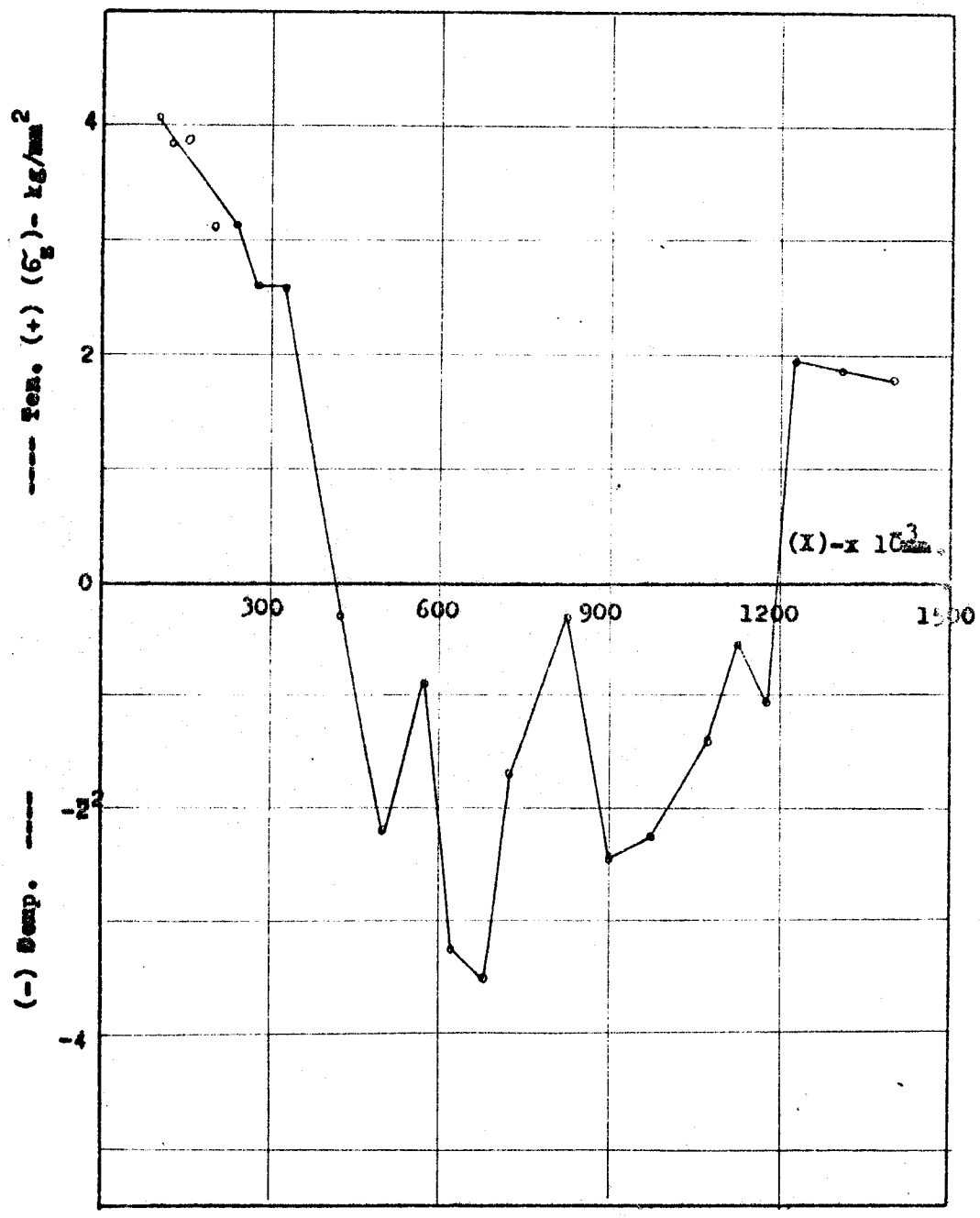

Fig. (13) Longitudinal Residual Stress, (σ_s)- kg/mm^2 Vs. Sub-Surface Depth, (X)-10^{-3} mm. For α = 30°, N = 1600 R.P.M. and t = 6mm.

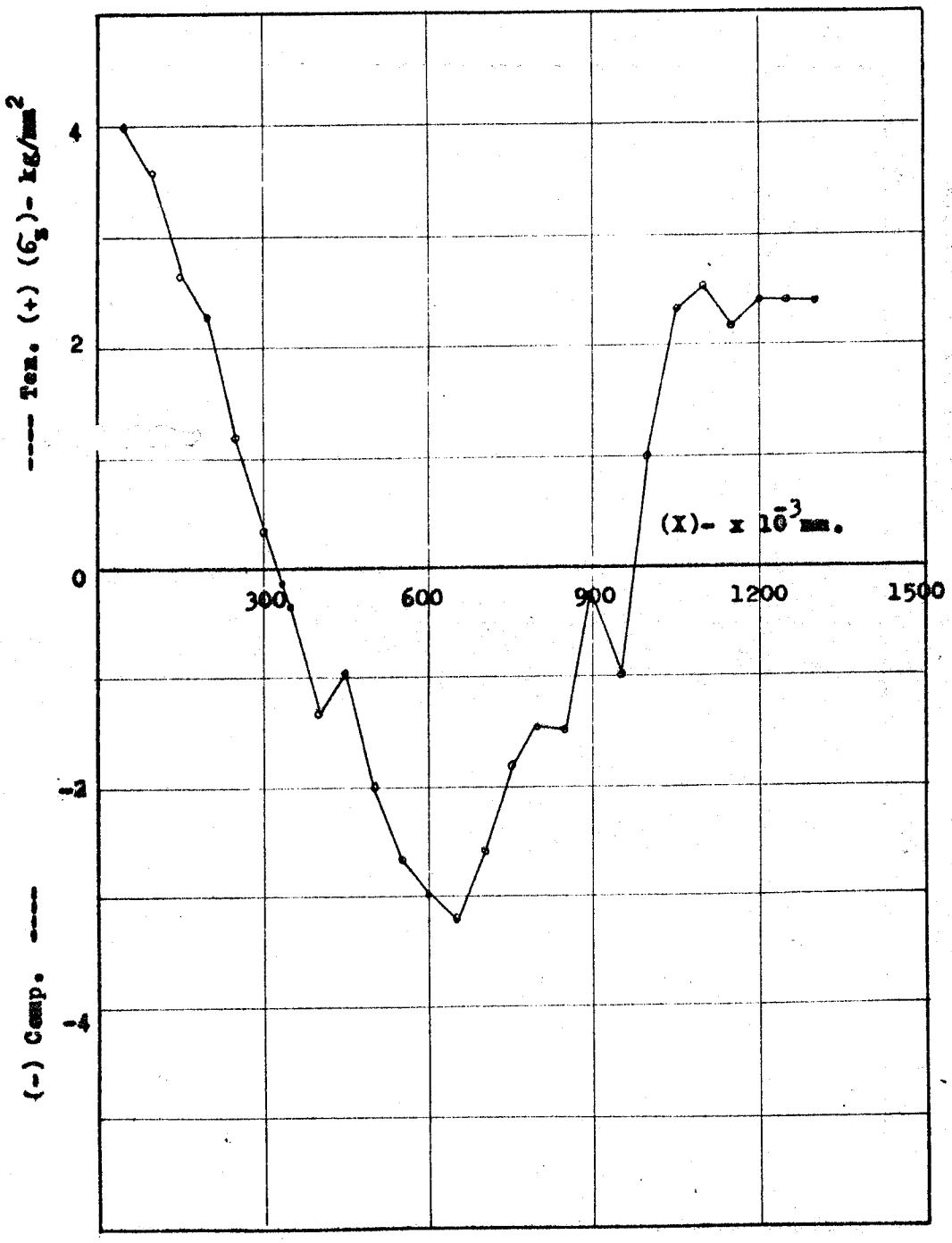

Fig. (14) Longitudinal Residual Stress, ($\bar{6}_x$)- kg/mm^2 Vs. Sub- Surface Depth, (X)- x 10^{-3} mm. For $\alpha = 60^0$, N = 1600 R.P.M. and t = 6 mm.

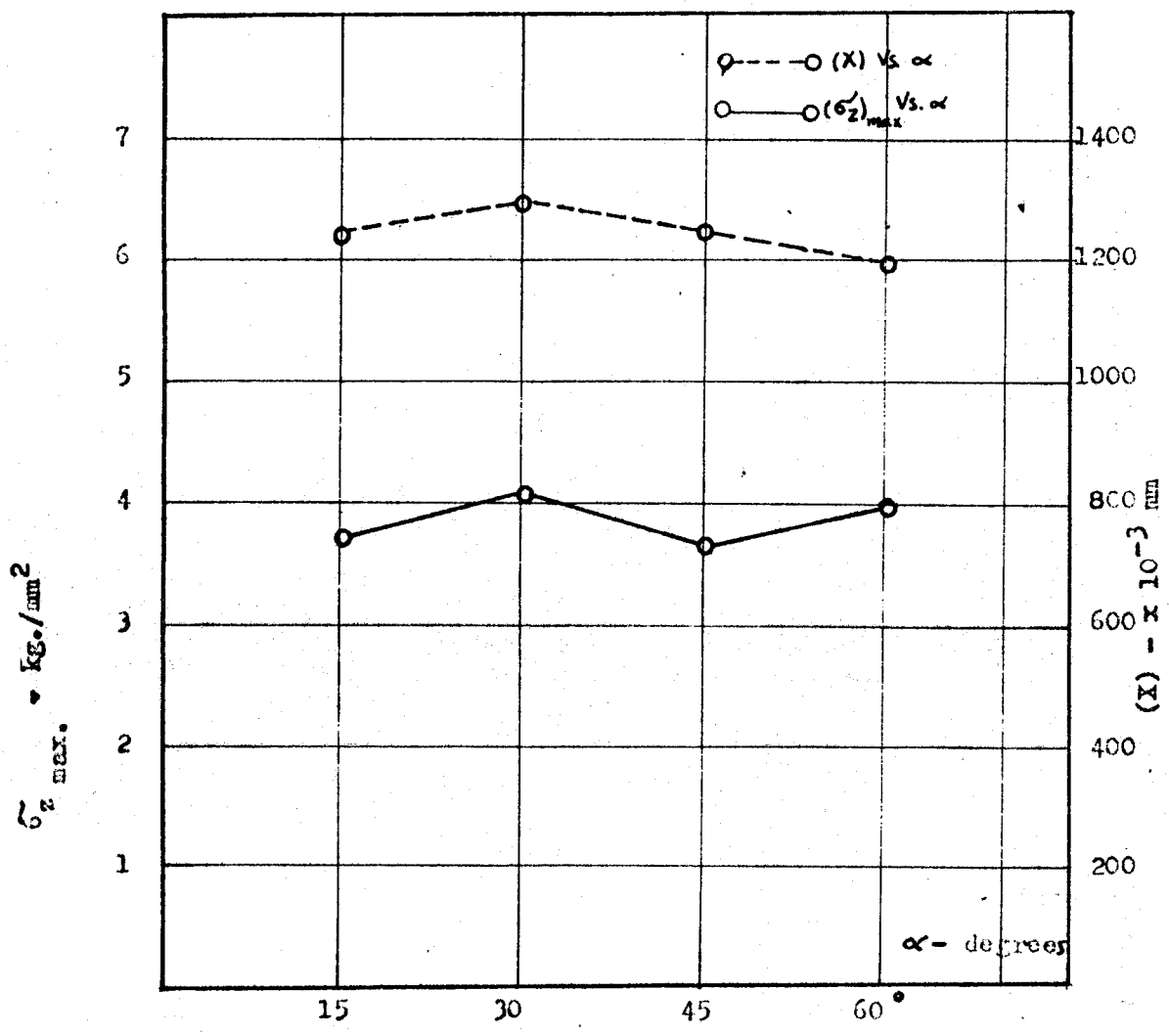

Fig. (15) Variation of the maximum Residual Stress, (σ_z) max. - kg./mm² and the Stressed Layer, (X)-x10^{-3} mm with the Chamfering angle, (α) - degrees.

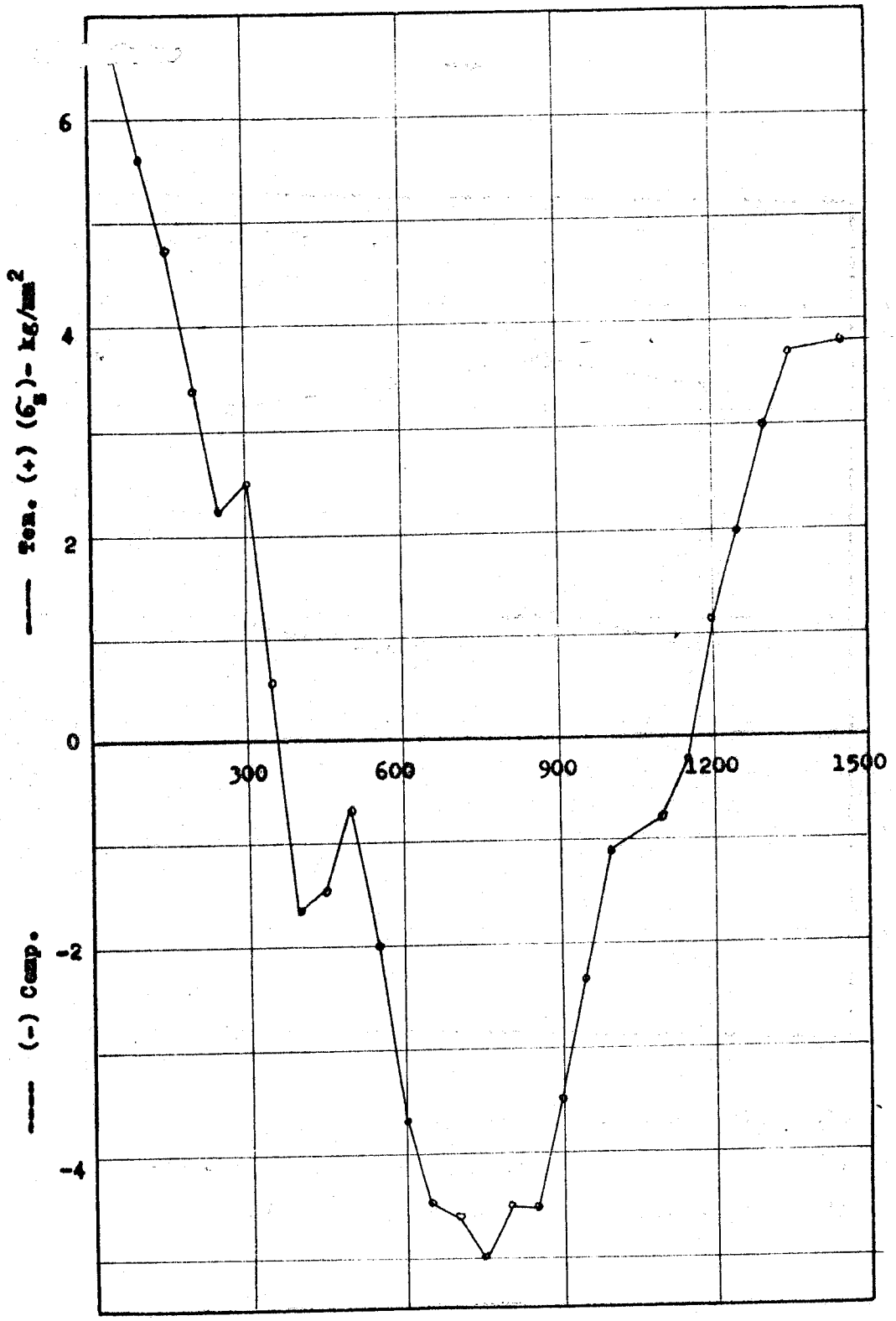

Fig. (16) Longitudinal Residual Stress, (σ_g)- kg/mm^2 Vs. Sub-Surface

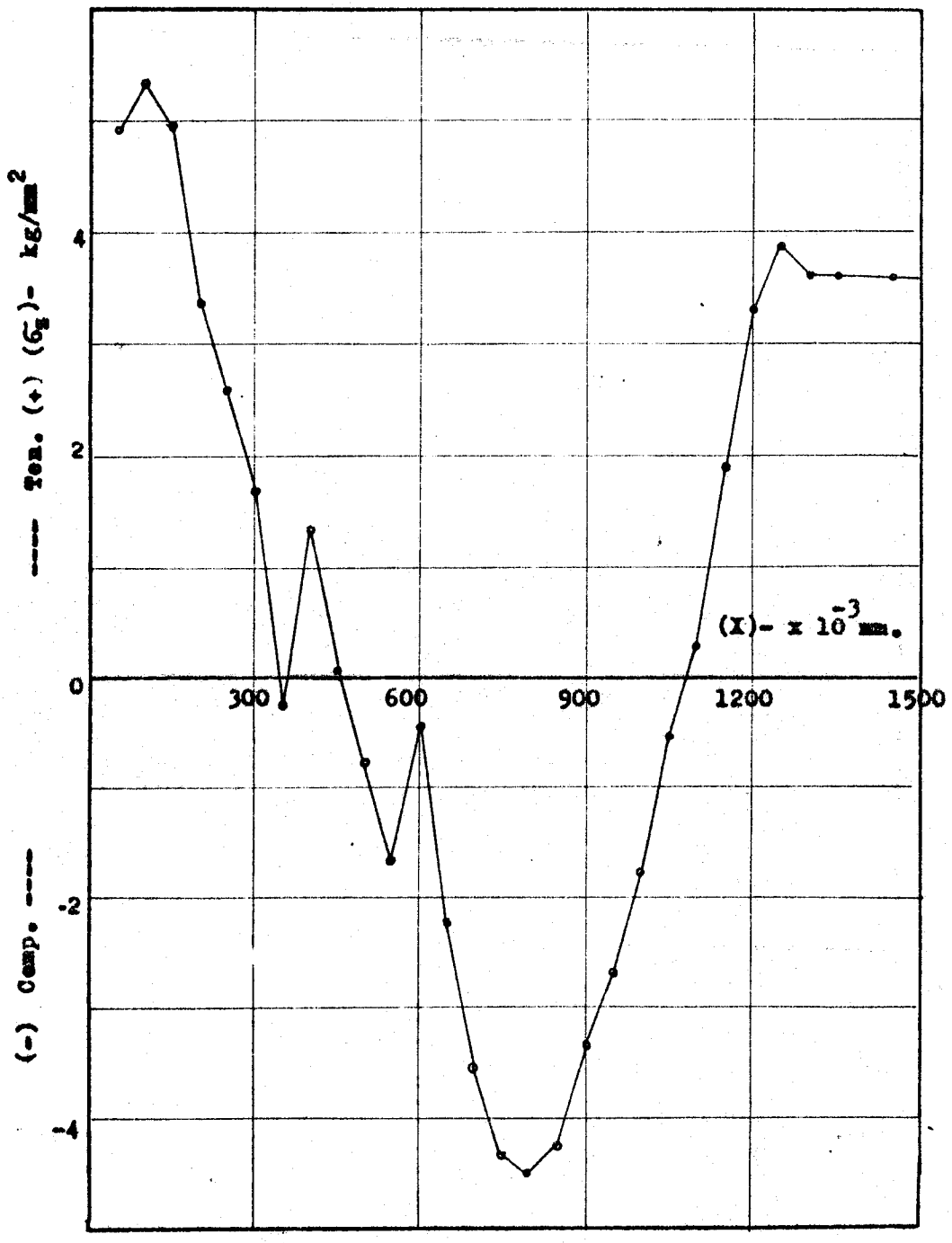

Fig. (17) Lengitudinal Residual Stress, (σ_x)- kg/mm^2 Vs. Sub-Surface, (X)- x 10^{-3} mm. For t = 5 mm, N = 1600 R.P.M. and α = 45° .

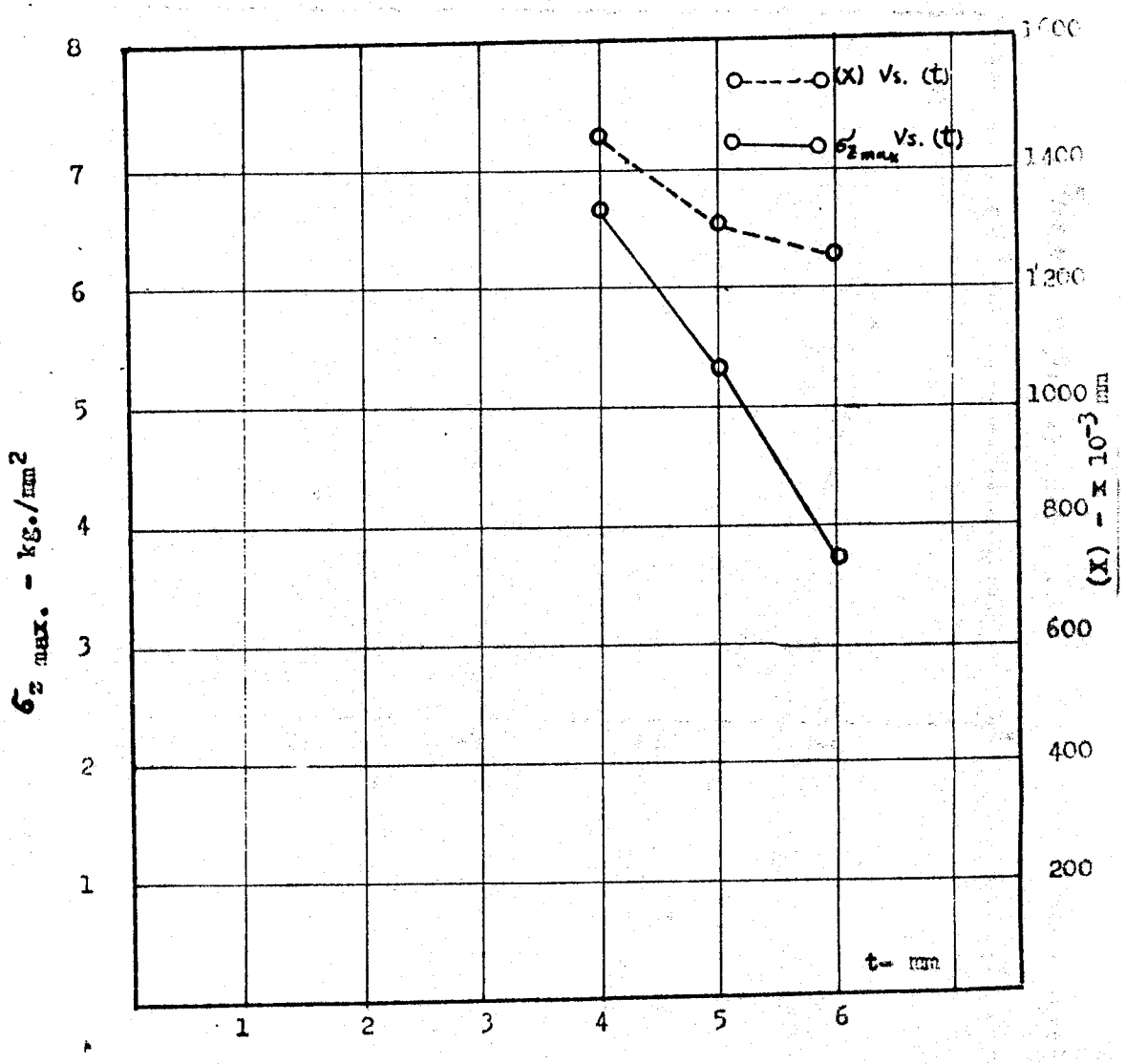

Fig.(18) Variation of the maximum Residual Stress, (σ_z) max - Kg./ mm^2 and the Stressed Layer, (X)-x10^{-3}mm with the Tube wall thickness, (t) - mm.

تقرير الاجهادات المتخلفة فى انابيب الألمنيوم الملحومة بالاحتكاك

د ٠ منصور السيد عبد المنعم د ٠ سعاد محمد سراج ا ٠د ٠عبد الهادى ناصر م ٠عادل عبد العزيز

يتعرض هذا البحث الى دراسة بعض أساسيات عملية اللحام الاحتكاكى لأنابيب الألمنيوم النقى تجاريا ٠٠

وقد تم فى هذه الدراسة تطويع مخرطة الزنبة كى تجرى بواسطتها عمليات اللحام المطلوبة وقد استلزم ذلك العديد من المحاولات حتى أمكن التوصل الى تصميم مناسب لترشيد انابيب الألمنيوم النقى (٩٩٫٦٪) أثناء أداء اللحام على المخرطة وكانت متغيرات البحث سرعة دوران المخرطة ـ تخانة ـ الأنابيب المستخدمة ـ وزاوية الشطف الرأسية لنهايات الأنابيب ٠٠

وقد تم تقدير الاجهادات المتخلفة فى القطع المتوسط للأنبوبة الملحومة بواسطة طريقة ازالة الطبقة المجهدة (Stressed Layer Removal) ٠٠

تمت عملية الازالة باستخدام حدود قطع عمودية شديدة الرهافة (Very Sharp Edge) مع التبريد الغزير أثناء عملية الازالة للتقليل ماأمكن من الاجهادات المتخلفة التى قد تنتج من عملية القطع نفسها ٠

وعلى العموم فعندما زادت سرعة عمود المخرطة زادت قيمة ـ اجهادات الشد المتخلفة وزاد عمق الطبقة المجهدة ٠

وكلما زاد سمك الأنبوبة الملحومة كلما زادت قيمة الاجهادات المتخلفة وعمق الطبقة المجهدة ٠

بينما لم يكن هناك تاثيرات كبيرة عند تغيير زاوية الشطف الرأسية وقد وجد ان سمك الطبقة المجهدة يتراوح مابين ١١٥٠ ، ١٣٣٠ ميكرون والتى تمثل نسبة قدرها من ٠٫٢ الى ٠٫٣٥ من سمك الأنبوبة ٠

وعن طبيعة الاجهادات الناتجة فقد كانت اجهادات شد أولا تلتها اجهادات ضغط ثم تبعتها اجهادات شد ٠

وقد وجد ان المساحة المحصورة تحت اجهادات الشد تقارب المساحة المحصورة تحت اجهادات الضغط ٠